Final Report: Evaluation and Improvement of Ocean Model Parameterizations for NCEP Operations

PI: Dr. Lynn K. Shay
Co-PI: George Halliwell
NCEP Collaborator(s): Drs. Hyun-Sook Kim and Carlos Lozano

RSMAS/MPO, University of Miami – 4600 Rickenbacker Causeway, Miami, FL 33149, USA
Phone: (305) 421-4075 - Fax: (305) 421-4696 - Email: nick@rsmas.miami.edu –
Internet: http://isotherm.rsmas.miami.edu/~nick

Goal: The long term goal of this NOAA Joint Hurricane Testbed (JHT) grant is to evaluate and improve ocean model parameterizations in NOAA National Centers for Environmental Prediction (NCEP) coupled hurricane forecast models in collaboration with the NOAA Tropical Prediction Center (TPC) and NOAA/NCEP Environmental Modeling Center (EMC). This effort targets the Joint Hurricane Testbed programmatic priorities **EMC-1** and **EMC-2** along with hurricane forecaster priorities **TPC-1** and **TPC-2** that focus on improving intensity forecasts through evaluating and improving oceanic boundary layer performance in the coupled model and improving observations required for model initialization, evaluation, and analysis. This project will be conducted under the auspices of the Cooperative Institute of Marine and Atmospheric Science program, and addresses **CIMAS Theme 2 and 3: Tropical Weather and Sustained Coastal and Ocean Observations and NOAA Strategic Goal 3: Weather and Water (local forecasts and warnings)**.

Specific objectives of this grant are:

i) optimizing spatial resolution that will permit the ocean model to run efficiently as possible without degrading the simulated response;
ii) improving the initial background state provided to the ocean model;
iii) improving the representation of vertical and horizontal friction and mixing;
iv) generating the realistic high-resolution atmospheric forcing fields necessary to achieve the previous objectives; and
v) interacting with NOAA/NCEP/EMC in implementing ocean model code and evaluating the ocean model response in coupled hurricane forecast tests.

Summary of Progress and Recommendations: This effort has proceeded along two closely related tracks: (1) evaluation of ocean model performance; and, (2) the preparation and analysis of the *in-situ* ocean observations required to perform these careful evaluations. The Hybrid Coordinate Ocean Model (HYCOM) is chosen as the primary ocean model because it is being evaluated as the ocean model component of the next-generation coupled hurricane forecast model at NOAA/NCEP/EMC. It also contains multiple choices of numerical schemes and subgrid-scale parameterizations, making it possible to isolate model sensitivity to individual processes and devise strategies to improve model representation of these processes. Results from our model evaluation during Hurricane Ivan (2004) were recently published (Halliwell *et al.*, 2011), leading to a specific list of model recommendations. Reference experiments have also been performed for Hurricanes Katrina and Rita (2005).

A key result of our prior work is that accurate ocean model initialization with respect to both the location of ocean features and the upper-ocean temperature and salinity (density) profiles within them is the most important factor influencing the quality of SST and intensity forecasts from coupled models. The initialization errors and biases encountered in our previous work produced large SST forecast errors that made it impossible to quantitatively estimate optimum values of ocean model and surface flux parameterizations. As a result, the modeling effort over the prior year has primarily focused on improving ocean model initialization and developing useful metrics to evaluate model performance. Multiple ocean analysis products produced by operational forecast centers that use HYCOM and other model types have been evaluated for overall accuracy, and also to quantify the impact of targeted airborne ocean observations on the accuracy of initial ocean fields. The accuracy of velocity shear profiles produced by HYCOM, which are critically important for simulating entrainment cooling of SST, has been further evaluated against the measurements available during Hurricane Ivan.

What separates this modeling study from others is a fairly complete analysis of experimental data sets. This observational effort has included processing the *in-situ* Acoustic Doppler Current Profiler (ADCP) data from Ivan (provided by the U.S. Naval Research Laboratory). It also included moored observations during Katrina and Rita (data courtesy of Bureau of Ocean Energy Management Regulation and Enforcement (BOEMRE: formerly Minerals Management Service-MMS), and the NOAA Hurricane Research Division (HRD) Intensity Fluctuation Experiments (IFEX) 2005 observations for pre- and post Rita (Rogers *et al.*, 2006; Jaimes and Shay, 2009, 2010). In addition, oceanic and atmospheric profiler measurements were acquired during hurricanes Gustav and Ike in 2008 in and over the Gulf of Mexico. In all of these cases, satellite observations (altimetry and SST) have been obtained and Ocean Heat Content (OHC) maps have been produced following the Shay and Brewster (2010) approach. The effort to improve ocean model initialization during the previous year was significantly enhanced by the large set of ocean observations in the Gulf of Mexico collected in response to the Deepwater Horizon oil spill. Since early May of 2010, both Shay and Halliwell redirected part of their work toward observational and modeling efforts in response to the spill, which included the acquisition of multiple synoptic maps of upper-ocean temperature, salinity, and velocity profiles deployed from NOAA WP-3D aircraft. These repeat flights in conjunction with other *in-situ* observations provide an unprecedented dataset for evaluating existing analysis products for ocean model initialization.

Based on our work over the prior year, we conclude that data-assimilative ocean model analysis products will achieve sufficient accuracy to replace the existing operational feature-based initialization procedure. Model evaluation conducted in the Gulf of Mexico demonstrates that the Navy global HYCOM analysis is presently the optimum choice to provide initial fields for ocean model initialization. The large negative temperature bias present in the Navy HYCOM products that we documented in prior reports and publications has been substantially corrected by employing a different vertical projection procedure to estimate synthetic temperature and salinity profiles from satellite altimetry for assimilation. By contrast, significant problems were encountered in the NOAA/EMC HYCOM-based RTOFS Atlantic Ocean analysis, and also in the existing operational feature-based initialization procedure. As discussed later in this report, the

Navy will soon release a HYCOM reanalysis product using this latest forecast system, which will enable us to revisit historical storms with improved initial fields. We further determined that assimilation of P-3 synoptic ocean profiles in the eastern Gulf of Mexico reduced upper-ocean temperature RMS errors by ~30% and remaining biases by ~50%. Given the improvement achieved in this particular case, research on the optimum use of targeted aircraft observations to improve ocean model initialization must continue. Finally, our research demonstrates the critical importance of using three-dimensional ocean models that include the impact of ocean dynamics on the magnitude and pattern of SST cooling. Results supporting these conclusions are summarized in the remainder of this report.

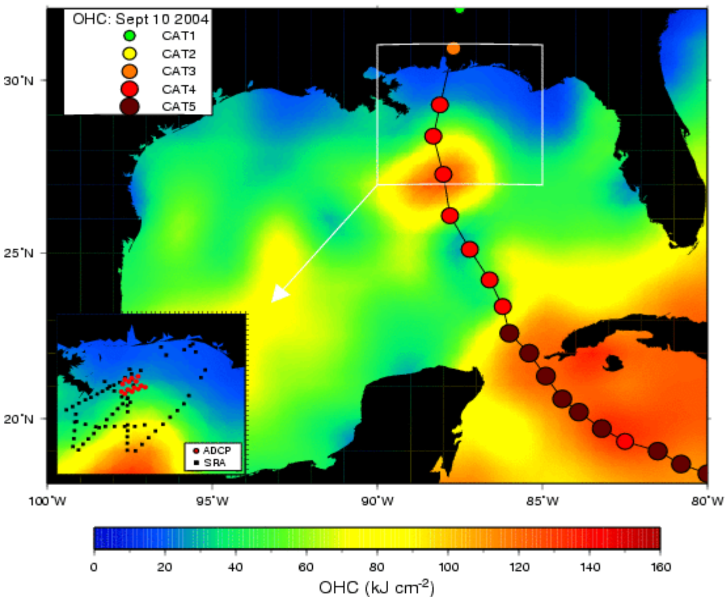

Figure 1: *OHC map and inset showing NRL mooring locations (red) and SRA wave measurements (black) relative to Ivan's storm track and intensity. The OHC pattern shows the WCR encountered by Ivan prior to landfall. The cooler shelf water (OHC < 20 kJ cm^{-2}) resulted from the passage of Frances two weeks earlier*

Current Profiler Analysis During Ivan: Hurricane Ivan passed directly over 14 ADCP moorings (Figure 1) that were deployed from May through Nov. 2004 as part of the NRL *Slope to Shelf Energetics and Exchange Dynamics (SEED)* project (Teague *et al*., 2007). These observations enable the simulated ocean current (and shear) response to a hurricane over a continental shelf/slope region to be evaluated. These profiler measurements provide the evolution of the current (and shear) structure from the deep ocean across the shelf break to the continental shelf. The current shear response, estimated over 4-m vertical scales, is shown in Figure 2 based on objectively analyzed data from these moorings. The normalized shear magnitude forced by Ivan is a factor of four times larger over the shelf (depths < 100 m) compared to normalized values over the deeper part of the mooring array (500 to 1000 m). The current shear rotates anticyclonically (clockwise) in time, consistent with the forced near-inertial response (periods slightly shorter than the local inertial period). In this measurement domain, the local inertial period is close to the 24 hr diurnal tide period. By removing the weaker tidal currents and digitally filtering the records, the analysis revealed that the predominant response was due to forced near-inertial motions. These motions have the characteristic time scale for the phase of each mode when the wind stress scale ($2R_{max}$~64 km in Ivan during time of closest approach) exceeds the deformation radius associated with the first baroclinic mode (≈ 30 to 40 km). This time scale increases with the number of baroclinic modes because phase speeds decrease with increasing mode number (Shay *et al.*, 1998). The resulting vertical energy propagation from the OML into the ocean interior is associated with the predominance of the anticyclonic (clockwise) rotating energy with depth and time that is about four times larger than the cyclonic (counterclockwise) rotating component.

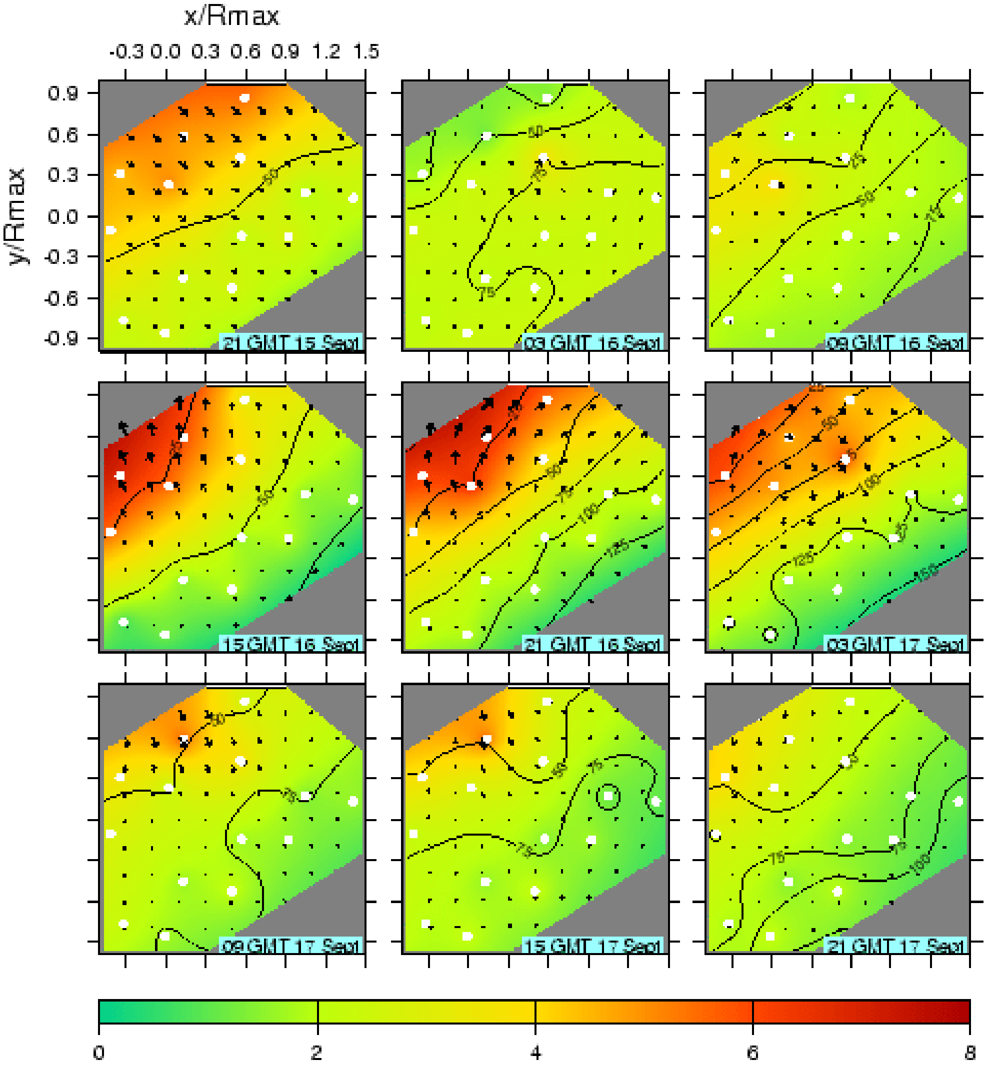

Figure 2: *Spatial evolution of the rotated current shear magnitude normalized by observed shears from the ADCP measurements (white dots) normalized by observed shears in the LC of 1.5 x* 10^2 s^{-1} *(color) during Ivan starting at 2100 GMT 15 Sept every 6 hours. Black contours (25-m) represent the depth of the maximum shears. Distances are normalized by* R_{max} *(32 km for Ivan).*

Observed current shear profiles were estimated over 4-m vertical scales for each time sample following hurricane passage at mooring 9 (Figure 3). The shear magnitudes are typically two to three times larger than observed in the Loop Current (e.g., during Lili's passage). This is not surprising since the SEED ADCP measurements were acquired in the Gulf Common Water (Nowlin and Hubertz, 1972), and they are similar to the shear documented during hurricane Gilbert's passage where up to 3.5°C cooling was observed in the Gulf Common Water. In the near-inertial wave wake (Shay *et al.*, 1998), the key issue is how much of the current shear is associated with near-inertial wave processes. Compared to the Gulf Common Water, the presence of warm and cold eddies significantly impact these levels of near-inertial wave (and shear) activity (Jaimes and Shay, 2010).

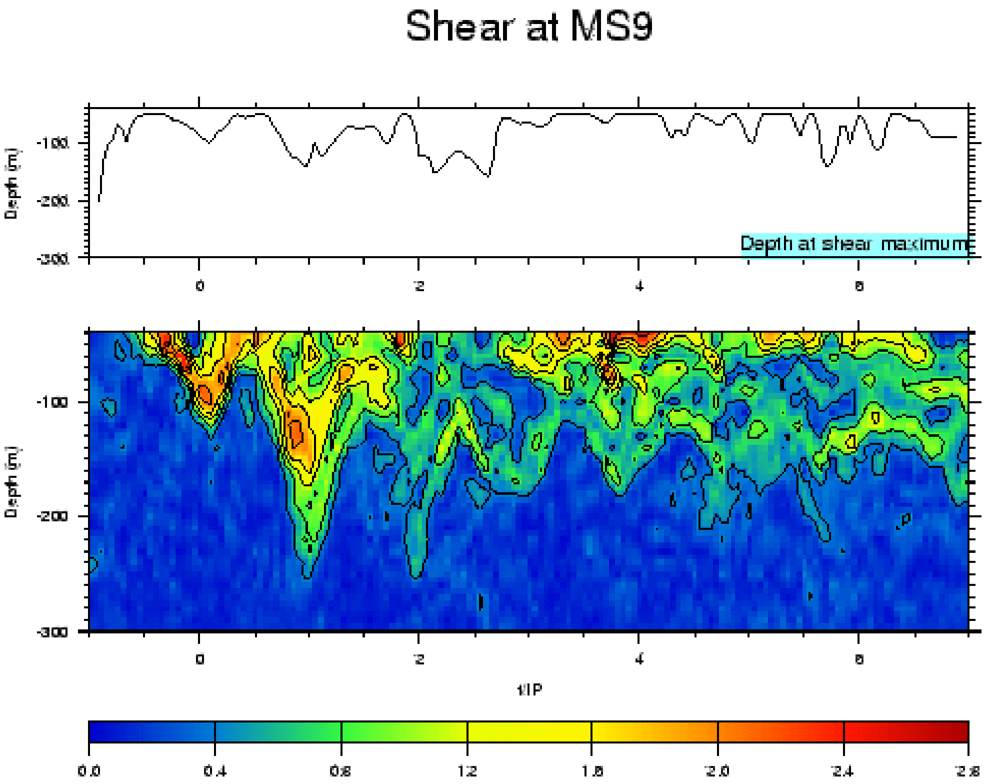

Figure 3: *Time series (normalized by inertial period) of observed current shear magnitudes (colored contours) and the respective depths (m) of maximum current shears observed at Mooring 9 (1.5* R_{max} *to the right of the Ivan) relative to the time of the closest approach. Shears are normalized by a value of 1.5 x* 10^{-2} s^{-1} *that have been observed in the LC (Shay and Uhlhorn, 2008).*

Comparison of Model and Observed Current Shear: At SEED mooring 9, velocity shear magnitude profiles from a control experiment are compared to shear profiles from alternate experiments that each varies a single attribute (Figure 4). These observations and simulations suggest that vertical energy propagates out of the surface mixed layer and into the thermocline consistent with surface intensified flows (Jaimes and Shay, 2010). The closest visual agreement exists between observed shear and simulated shear from the control experiment that used KPP vertical mixing and the Donelan *et al.* (2004) wind stress drag coefficient. Velocity shears produced by two different vertical mixing models (Mellor-Yamada and GISS) and by two different choices of wind stress drag coefficient (Powell *et al.*, 2003; Large and Pond capped at high wind speed) produced less realistic shear responses in comparison to observations. These latest results agree with the recommendations of the Ivan analysis in Halliwell *et al.* (2011) as listed in Table 1. We are in the process of making additional comparisons for all the ADCP records during storm forcing. The importance of the impact of vertical missing and wind stress drag coefficient on shear evolution and the resulting entrainment of cold water into the mixed layer (and hence SST cooling rate) cannot be overstated.

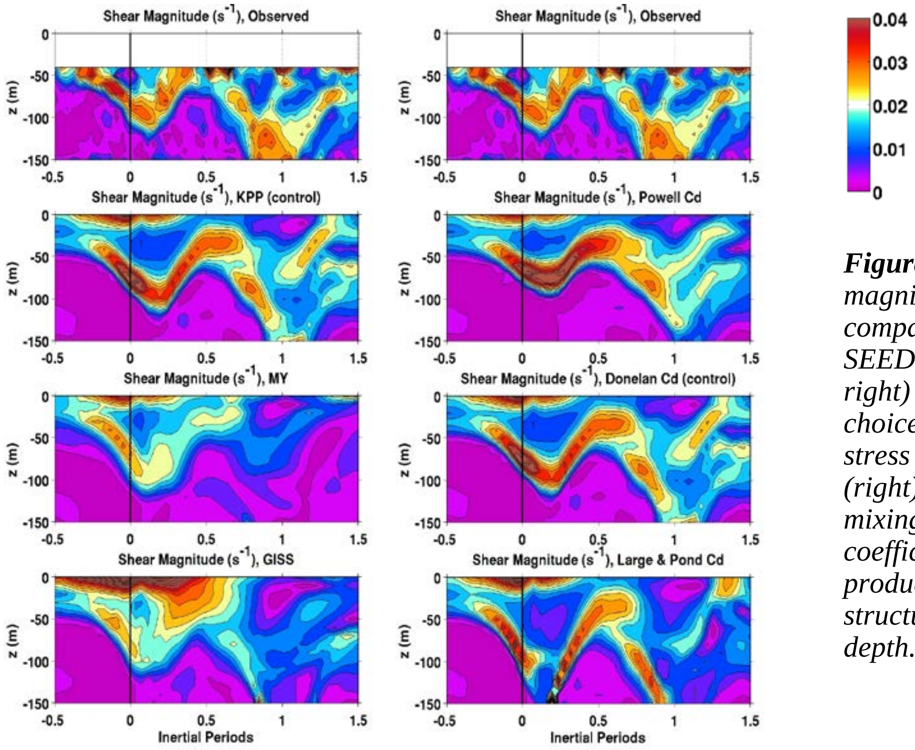

Figure 4*: Time series of the magnitude of vertical shear (s^{-1}) comparing observations from SEED mooring 9 (top left and top right) to three vertical mixing choices (left) and three wind stress drag coefficient choices (right). The combination of KPP mixing and Donelan et al. drag coefficient parameterizations produce the most realistic shear structure and maximum OML depth.*

Model Attribute	**Recommendations**
Horizontal resolution	≈10 km adequately resolves horizontal structure of response forced by eye/eyewall
Vertical resolution	≈10 m in the OML is adequate to resolve vertical structure of shear
Vertical mixing	KPP outperformed the other models; MY, GISS produce slower cooling, larger heat flux, less-accurate shear representation
C_D	Donelan, Large & Pond capped, Jarosz *et al.* (values between 2.0 and 2.5x10^{-3} at high wind speed) produce most realistic results
C_{EL}, C_{ES}	Little SST and velocity sensitivity but large heat flux sensitivity. Need heat flux observations to evaluate
Atmospheric forcing	Must resolve inner-core structure (≤10 km horizontal resolution)
Outer model (assimilative vs. non-assimilative)	Accurate initialization is the most important factor to accurately forecast velocity and SST evolution in the GOM and NW Caribbean
Ocean dynamics (1-D vs. 3-D)	3-D required (second most important factor in the GOM)

Table 1*: Recommendations to improve upper-ocean forecasts during tropical cyclones based on analysis of the simulated ocean response to Hurricane Ivan in the Gulf of Mexico (Halliwell et al., 2011).*

Analysis of Feature-Based Initialization: A major goal of this project is to interact with the HWRF developers at EMC and URI to evaluate the performance of ocean models to be used in the next-generation HWRF model and to improve the performance of the ocean model. As part of this effort, URI provided feature-based initialization fields to G. Halliwell initially to be used to initialize HYCOM in a POM-HYCOM comparison study. By inspecting these fields, we discovered a problem that will impact the pattern and rate of SST cooling in the vicinity of the Loop Current and warm eddies as represented by the feature-based algorithm (Falkovich *et al.*, 2005).

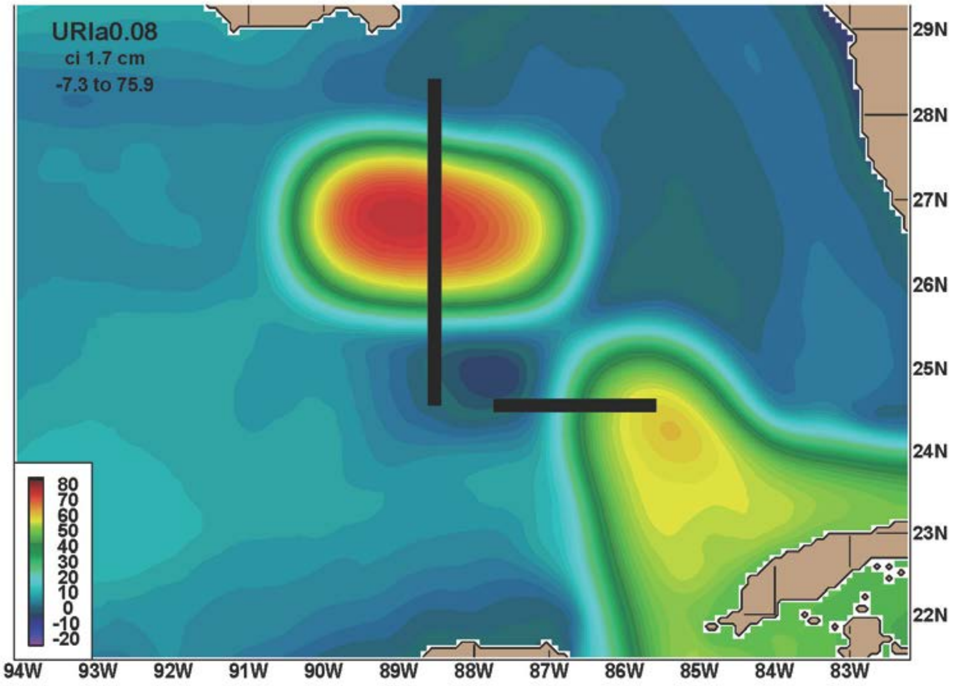

Figure 5. *Pre-Ivan initial SSH map derived from the feature-based ocean model initialization product. The two cross-sections presented in Figure 6 are illustrated with black bars.*

The primary problem is described as follows: Baroclinic fronts slope in the wrong direction with increasing depth. This situation is illustrated by initial HYCOM fields prior to hurricane Ivan produced from the feature-based product and spun up for several inertial periods to approximately achieve geostrophic balance. Figure 5 shows the SSH pattern in the Gulf of Mexico, highlighting the LC Path and the detached warm ring. The subsurface structure of these features is investigated along the two sections shown in Figure 5. A meridional cross-section of zonal velocity through the warm ring (Figure 6) reveals that the diameter of the ring *increases* with increasing depth instead of decreasing as expected. Similarly, a zonal cross-section of meridional velocity across the Loop Current north of the Yucatan Channel (Figure 6) demonstrates that the core of maximum velocity shifts *westward* with increasing depth instead of eastward as expected. In both of these sections, the model interfaces below the near-surface level-coordinate domain follow isopycnals and demonstrate that the fronts (large horizontal density gradient and vertical shear) slope in the wrong direction with increasing depth. There is also a problem in blending the ring with the background ocean structure that is caused by a large vertical density jump near 650 m depth in the ring interior.

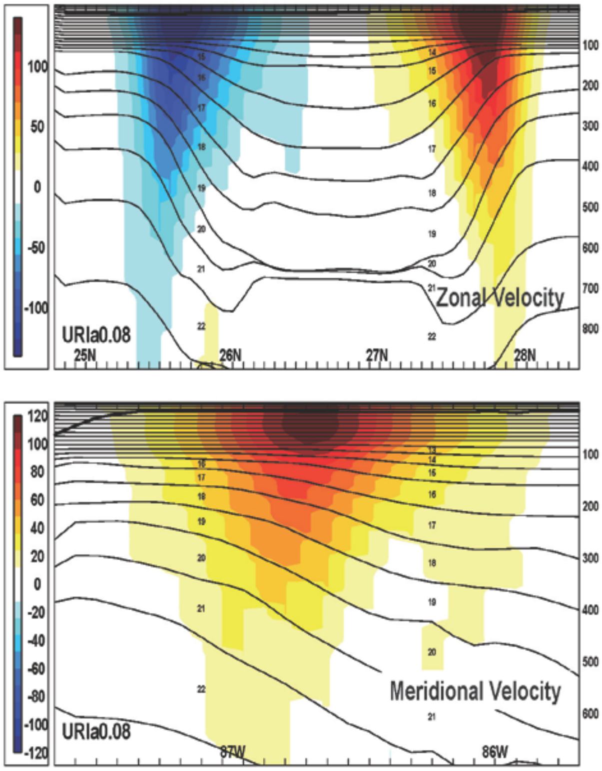

Figure 6. *Pre-Ivan velocity cross-sections: (top) zonal velocity from a meridional section through the detached ring and (bottom) meridional velocity from a zonal section across the Loop Current. The locations of these two cross-sections are illustrated in Figure 5.*

Table 2: *Summary of thirteen NOAA WP-3D aircraft flights on RF-42 in the eastern Gulf of Mexico from 24 to 28^{o}N and 85 to 89^{o}W in support of DWH oil spill that occurred on 20 April 2010 in the northern Gulf of Mexico along the slope of the DeSoto Canyon and IFEX flights . The overall success rate for all probes (in parentheses) was ~83%. This is lower than usual due to manufacturing problems with the AXCPs such as unsealed transmitter boards, agar, and software and firmware problems in the new Mark21/Mark10A software. The number of GPS sondes deployed was 78 (from Shay et al., 2011).*

Flight	Event	AXBT	AXCP	AXCTD	TOTAL
100508H	DWH	52 (46)	0	0	52 (46)
100518H	DWH	29 (28)	26 (10)	11 (10)	66 (48)
100521H	DWH	42 (41)	22 (11)	2 (2)	66 (54)
100528H	DWH	41 (37)	22 (12)	2 (1)	65 (50)
100603H	DWH	37 (33)	23 (9)	6 (6)	66 (48)
100611H	DWH	53 (48)	15 (10)	0	68 (58)
100618H	DWH	34 (23)	22 (11)	8 (7)	64 (41)
100625H	DWH	58 (53)	0	6 (6)	64 (59)
100709H	DWH	59 (54)	12 (11)	6 (3)	77 (68)
100724H	*T.S. Bonnie*	35(33)	0	0	35 (33)
100812H	*Test*	6 (6)	6 (5)	0	12 (11)
100909H	*Pre Matthew*	62 (58)	0	20 (17)	82 (75)
100924H	*Pre Matthew*	30 (30)	10 (5)	20 (20)	60 (55)
Total		538(490)	158 (84)	81 (72)	777 (646)

DeepWater Horizon Oil Spill: The effort to improve ocean model initialization has been significantly enhanced by the extensive observational dataset collected in response to the Deepwater Horizon oil spill. Shay was responsible for flying nine missions from the NOAA WP-3D research aircraft to sample the Loop Current and adjacent eddies over the eastern Gulf of Mexico by deploying AXBTs, AXCPs and AXCTDs and GPS sondes (~666 profilers) in support of oil spill forecasting (see Figure 7, Table 2) (Shay *et al.*, 2011). Much of this sampling grid was over the BOEMRE moorings deployed in support of the Loop Current Dynamics Study. Although the short-term effect of this emergency effort was to delay our underway analysis of storms other than Ivan (Katrina, Rita, Frances, Gustav, Ike), the repeated aerial sampling over the eastern GOM in conjunction with other observations provided an unprecedented dataset for evaluating ocean model products initialization. Furthermore, the emergency aircraft sampling revealed significant problems with many of the AXCP probes and with vendor supplied software and firmware that will lead to improved sampling in the future in support of IFEX and HFIP.

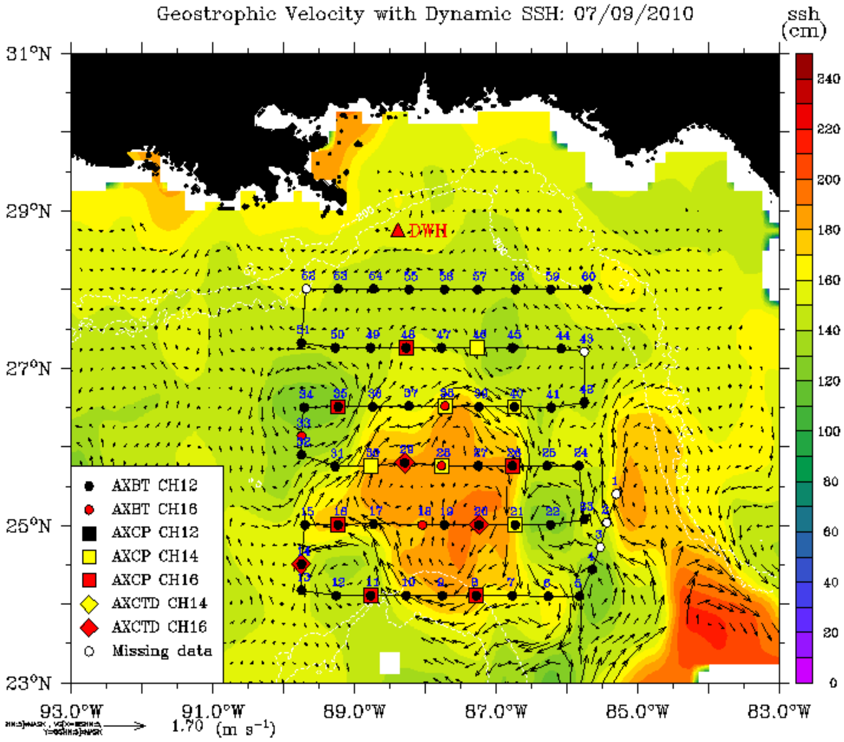

Figure 7: *NOAA WP-3D mesoscale ocean grid on 9 July 2010 deploying a combination of AXBTs (circles), AXCTDs (diamonds), and AXCPs (squares) superposed on sea surface height (cm: color bar) and surface geostrophic currents based on sea surface slopes (maximum vector is 1.7 m s^{-1}). Notice that warm core eddy (called Franklin) detached from the Loop Current.*

Our previous HYCOM evaluation efforts typically revealed large negative temperature biases in the upper ocean prior to nearly all storms (the Ivan bias was relatively small) that led to large overcooling when the model was initialized by these biased fields. The Navy recently changed their vertical T, S projection method from Cooper-Haines to "MODAS Synthetics" derived from their Modular Ocean Data Assimilation System. The P-3 profiles enabled us to quantify the improvement in upper-ocean temperature, and the new projection method was found to greatly reduce the mean bias and also reduce RMS errors by an average of ~50% (Figure 8). These observations also enabled us to evaluate several ocean analysis products for the purpose of ocean model initialization, and the Navy global HYCOM analysis product was determined to be the optimum choice with respect to both bias and RMS error (Figure 8). We conclude that errors and biases have been reduced to the point where data-assimilative ocean analyses should replace the feature-based method of ocean model initialization. By contrast, comparatively large errors and biases were evident in the NOAA/NCEP/EMC HYCOM-based RTOFS Atlantic Ocean analysis. We intend to work closely with EMC to insure that the ocean initialization scheme being implemented and tested for the HYCOM-HWRF coupled forecast model has errors comparable to or smaller than the Navy global HYCOM product.

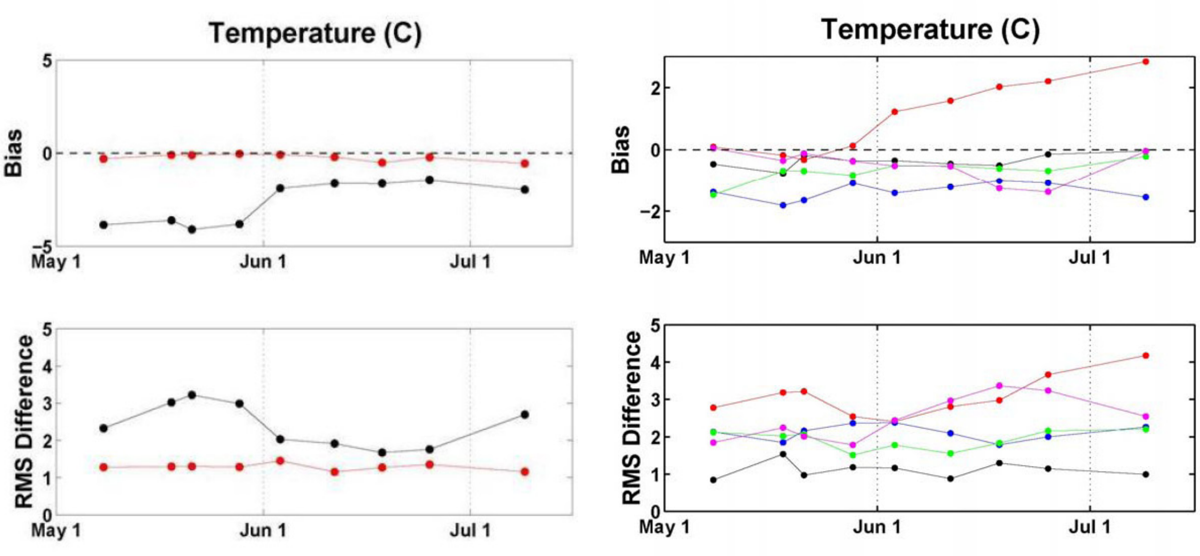

Figure 8: *Bias (top) and RMS error (bottom) between several ocean model analyses and P3 temperature profiles on nine flight days between 30 and 360 m. The left panels are for two HYCOM Gulf of Mexico analyses, one using the old Cooper-Haines vertical projection of T and S profiles (black) and the other using the new "MODAS Synthetics" method (red). The right panels compare the Navy global HYCOM analysis (black) to four other ocean analyses: NOAA/EMC RTOFS HYCOM (red), NRL IASNFS NCOM (blue), NOAA/NOS NGOM (magenta), and North Carolina State SABGOM ROMS (green).*

The DWH oil spill aircraft observations also gave us a chance to perform a preliminary study of the impact that targeted (and gridded) aircraft observations will have on improving ocean model initialization for hurricane forecasting. In collaboration with NRL-Stennis (Ole Martin Smedstad and Pat Hogan), we performed twin Observing System Experiments (OSE) where two data-assimilative analyses were performed in the Gulf of Mexico. The first experiment assimilated all observations while the second denied only the P-3 profiles. The degree to which the upper-ocean temperature distribution was improved is demonstrated by the zonal cross-section across the detaching Eddy Franklin on 21 May 2010 (Figure 9). Denial of the P-3 observations doubled the temperature differences within the central region of the eddy above about 250 m, and also doubled the error along the eastern boundary of the eddy. Assimilation of P-3 profiles apparently improved the location of the eastern boundary of the eddy. The reduction in temperature bias (not included in Taylor diagrams) over all nine P-3 flight days is about 50% on average while the reduction of RMS error is 25 to 30% (not shown).

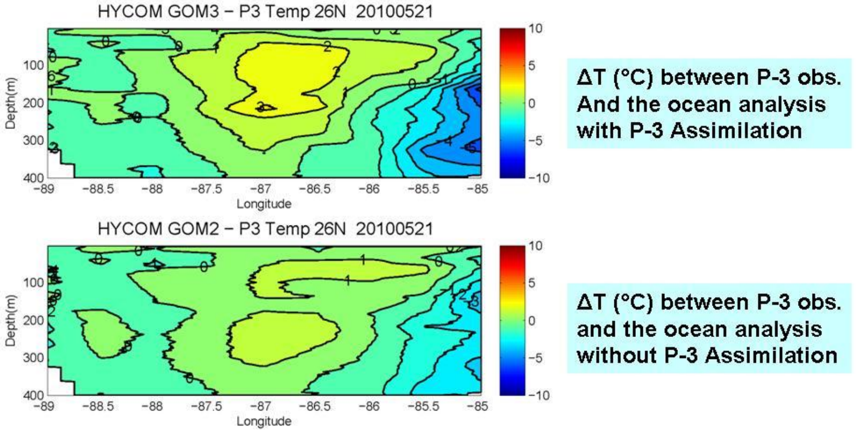

ΔT (°C) between P-3 obs. And the ocean analysis with P-3 Assimilation

ΔT (°C) between P-3 obs. and the ocean analysis without P-3 Assimilation

Figure 9: *Zonal temperature difference sections between P-3 temperature profiles along 25.5°N across the detaching Eddy Franklin on 21 May 2010 and two Gulf of Mexico HYCOM analyses, one that assimilated all observations (top) and one that denied only the P-3 observations (bottom) Assimilation of P-3 observations reduced errors by up to 50% in both the center and eastern boundary of the detaching eddy.*

A metric for evaluating ocean model analyses is utilized by comparing differing ocean model analyses to the observations using Taylor (2001) diagrams (Figure 10). These diagrams are first constructed by removing the overall mean from each field, normalizing each field by the variance of the observed field, and then calculating the three different but related metrics represented on this diagram (correlation coefficient, RMS amplitude, and RMS error). Errors are analyzed for two fields over all nine flight days: temperature between depths of 30 and 360 m from the aircraft and model profiles sampled at the same locations; and, horizontal maps of H_{20} calculated from these model and observed profiles (lower panel of Figure 10). To provide a reference point to assess analysis improvements resulting from data assimilation, a non-assimilative HYCOM experiment was also compared to observations, with the large black circles in the Taylor diagrams demonstrating the poor comparison between this numerical experiment and observations. Comparisons between seven data-assimilative ocean analyses and observations demonstrate that substantial error reductions result from assimilation of these observations, although the levels of error reduction varies among models. The model with the least error reduction (RTOFS-HYCOM: *Mehra and Rivlin* (2008)) is known to have a problem with their version of the model that will be fixed during the next upgrade of the operational system (*H. Tolman*, 2011, personal communication). Four models with intermediate error reduction (SABGOM-ROMS, http://omgrhe.meas.ncsu.edu/Group/; IASNFS NCOM (*Ko et al*., 2008); NOAA/NOS NGOM http://www.nauticalcharts.noaa.gov/csdl/NGOM.html; and experiment GoM-HYCOM run for the OSE) did not assimilate the aircraft profiles. The two models that assimilated profile observations (global HYCOM (*Chassignet et al.*, 2007) and experiment P3-GoM-HYCOM) produced the analyses that resulted in the largest error reduction compared to the non-assimilative models, again demonstrating the positive impact of assimilating the aircraft observations. Based on these encouraging results, we recommend that targeted aircraft observations should be used to improve ocean model initialization, and that research should continue to further evaluate the impact of these observations and to devise observing strategies that will maximize this positive impact. These results depend on factors such as the ocean model, data assimilation method, and details of the assimilation cycle such as the observation time windows and whether it is performed in real-time versus delayed reanalysis mode. Further detailed studies must consider these factors and employ observations that were not assimilated (e.g., BOEMRE moorings) to determine the robustness of these conclusions.

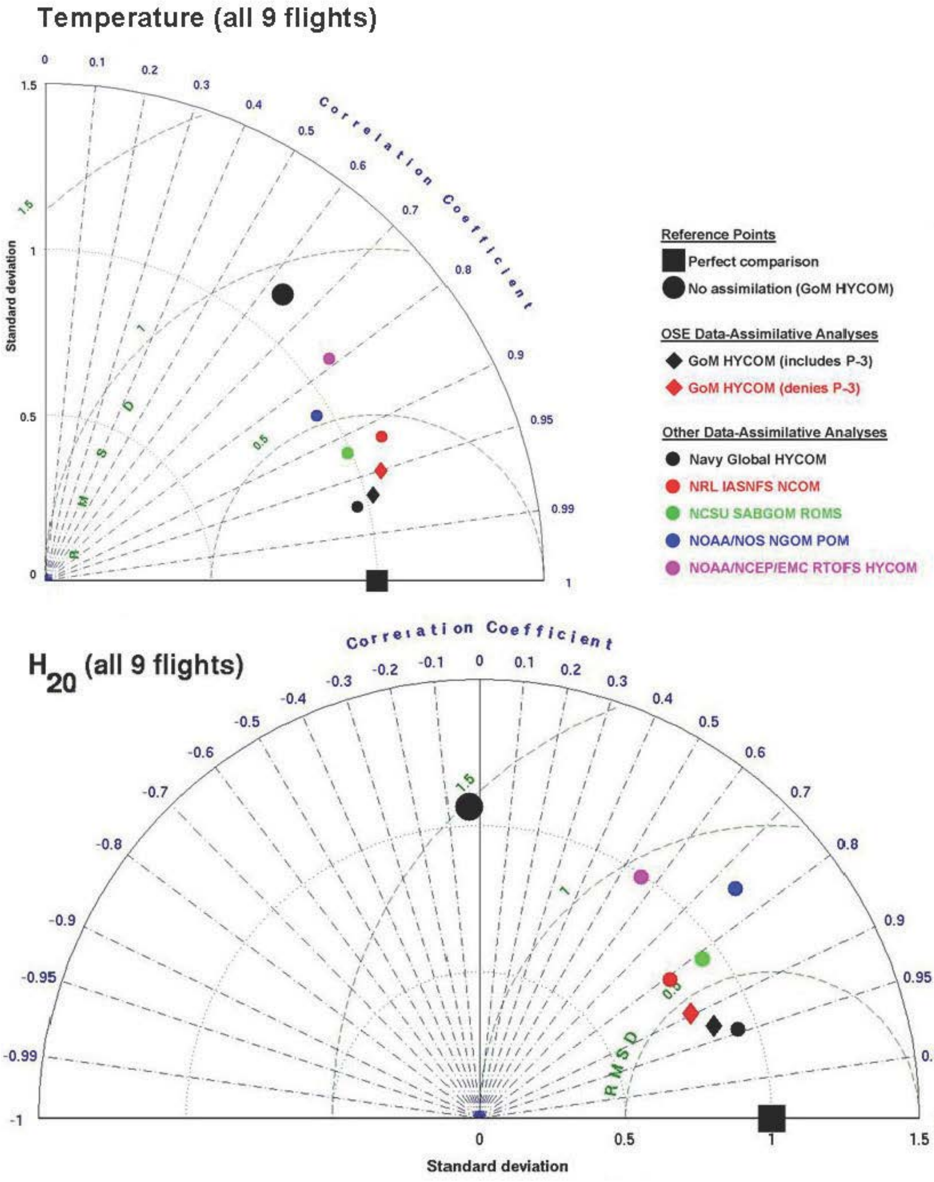

***Figure 10**. Taylor (2001) diagram metrics for (a) temperature (^{o}C) between 30 and 360 m depth and (b) H_{20} (m) comparing several model analyses to the observed fields. A perfect comparison is marked by the large black square. The quality of each analysis field is inversely proportional to the distance from this reference point. The large black circle represents a non-assimilative GoM HYCOM run. Black and red diamonds compare the P3-GoM-HYCOM and GoM-HYCOM experiments performed at NRL for the P-3 OSE. Analyses from several other models are included for comparison. The only two models that assimilated aircraft observations are P3-GoM-HYCOM (black diamond) and global HYCOM (small black circle).*

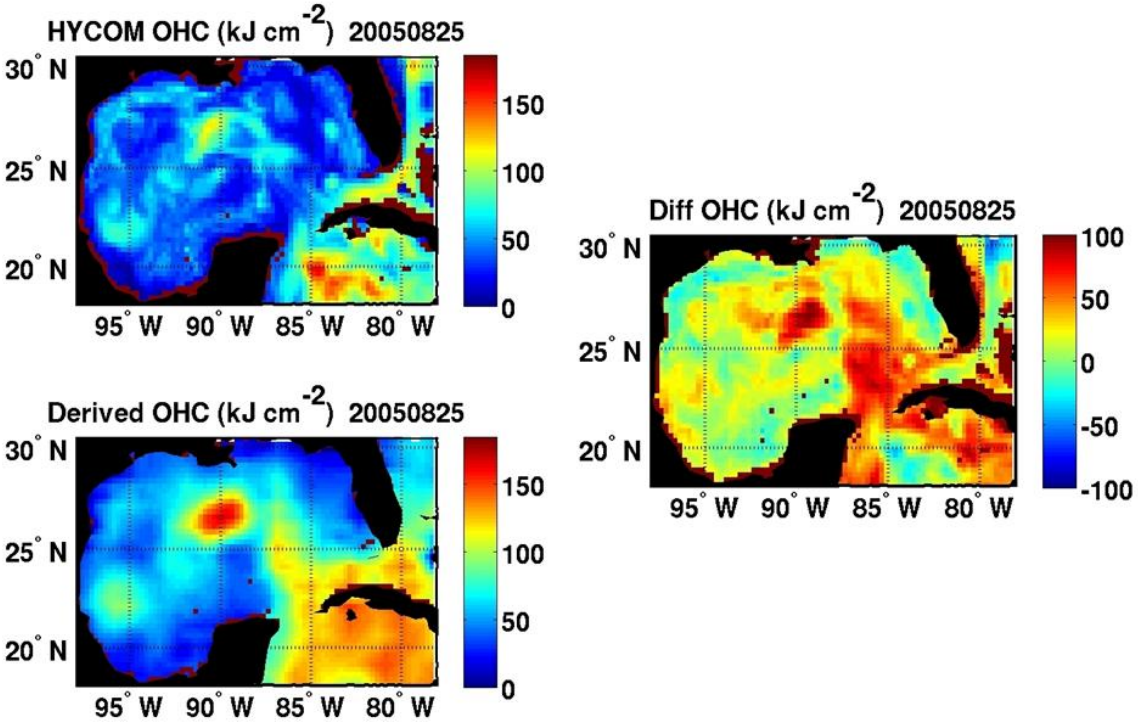

***Figure 11**. Ocean Heat Content relative to the 26°C isotherm prior to Hurricane Katrina on 25 August 2005. The left panels show OHC from the Navy HYCOM analysis (upper left) and derived from satellite altimetry, SST, and climatology (lower left; Mainelli et al., 2008). The right panel shows the difference between the two (derived minus model analysis).*

Katrina and Rita: Our original goal was to extend the analyses performed for Ivan to other storms, first to Katrina and Rita (2005) and then to Gustav and Ike (2008), to further evaluate model numerics and parameterizations. However, the Navy HYCOM analysis that we intended to use possessed very large cold biases in upper-ocean temperature that prevented accurate SST forecasts due to large overcooling. The bias is illustrated using Ocean Heat Content maps prior to Katrina (Figure 11). The Navy plans to produce a multi-decadal reanalysis using the updated nowcast-forecast system that reduced the large cold bias as shown in Figure 8 above. This new product was initially intended to be available by the beginning of 2011, so we decided to delay the model evaluation prior to other storms until it became available. Unfortunately, this new analysis was delayed and the product release is now scheduled for late 2011. We therefore proceeded with an observational and idealized model study of the impact of ocean features on upper-ocean SST cooling during Katrina and Rita using the predecessor model for HYCOM, the Miami Isopycnic-Coordinate Ocean Model (MICOM) (Jaimes *et al*., 2011). The decision to use MICOM was made to take advantage of the slab mixed layer model, which permits simplified analyses of mixed layer budgets.

The 3-D upper ocean thermal and salinity structure in the LC system was surveyed with Airborne eXpendable BathyThermographs (AXBT), Current Profilers (AXCP), and Conductivity-Temperature-Depth sensors (AXCTD) deployed from four aircraft flights during

September 2005, as part of a joint NOAA and National Science Foundation experiment (Rogers *et al.*, 2006; Shay, 2009). Flight patterns were designed to sample the mesoscale features in the LC system: the LC bulge (amplifying WCE), the WCE that separated from the LC about two days before the passage of Rita, and two CCEs that moved along the LC periphery during the WCR shedding event (Fig. 12). The first aircraft flight was conducted on 15 Sept (two weeks after Katrina or one week before Rita, i.e. pre-Rita), the second and third flights were conducted during Rita's passage (22 and 23 Sept, respectively), and the final flight was conducted on 26 Sept, a few days after Rita's passage. Pre-Rita and post-Rita (not shown) flights followed the same pattern, while these other Rita flights focused on different regions along Rita's track. Data acquired during pre-Rita includes temperature profilers from AXBTs, temperature and salinity profilers from AXCTDs, and current and temperature profilers from two AXCPs

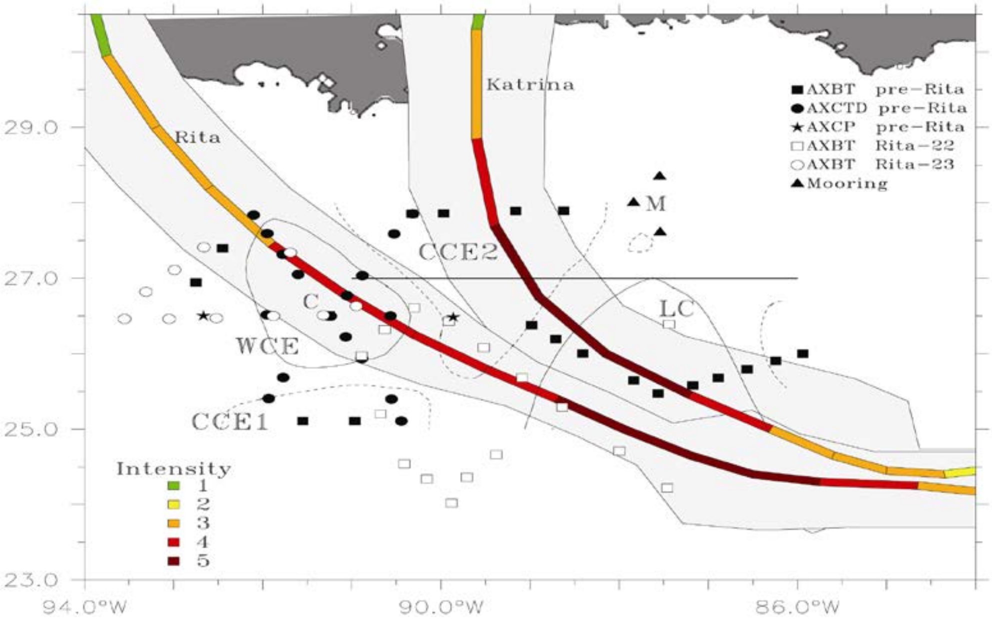

Figure. 12: *Airborne profilers deployed in Sept 2005 relative the track and intensity of Katrina and Rita (colored lines, with color indicating intensity as per the legend) over the LC System. The light-gray shades on the sides of the storm tracks represent twice the radius of maximum winds (R_{max}). The contours are envelops of anticyclonic (solid: WCE and LC) and cyclonic (dashed: CCE1 and CCE2) circulations. A set of AXBTs (not shown) was deployed after hurricane Rita (26 Sept), following a sampling pattern similar to pre-Rita (or post Katrina) (15 September). Point M indicates the position of several BOEMRE moorings used during this study, and Point C represents the drop site for profiler comparison (AXBT versus AXCTD). The transect along 27^{o}N indicates the extent of vertical sections discussed in the text (Jaimes and Shay, 2009).*

The combination of these airborne profiles of temperature and salinity measurements with the MMS-sponsored ADCP and CTD moorings were fairly consistent. These continuous measurements of ocean temperatures, salinities (via conductivities), and currents were acquired from the mooring sensors at intervals of 0.5 and 1 hr for CTDs and ADCPs, respectively. Although the moorings were located outside the radius of maximum winds R_{max} of hurricanes Katrina (~4.5 R_{max} where R_{max} = 47 km) and Rita (~17.5 R_{max} where R_{max} = 19 km) (Fig. 12), CCE2 that was affected by Katrina (category 5 status) propagated over the mooring site ≈2 days after interacting with the storm. The circulation of the LC bulge that interacted with Rita (category 5 status) extended over the mooring ≈3 days after having been affected by the storm. Cluster averages of the thermal structure revealed that the LC cooled by 1°C, the WCE temperature cooled by 0.5°C, and the eddy shedding region and the CCE cooled by more than 4.5°C (Jaimes and Shay, 2009). These profiles will represent a challenge for the model especially placing the oceanic features in the correct position as suggested by the Ivan model analyses (Halliwell *et al.,* 2011).

Jaimes and Shay (2010) analyzed the contrasting thermal responses during and subsequent to Katrina and Rita by estimating the energetic geostrophic currents in these oceanic features. Increased and reduced oceanic mixed layer (OML) cooling was measured following the passage of both storms over cyclonic (CCE) and anticyclonic (WCE) geostrophic relative vorticity ζ_g, respectively (Fig. 13). Within the context of the storms' near-inertial wave wake in geostrophic eddies, ray-tracing techniques in realistic geostrophic flow indicate that hurricane forced OML near-inertial waves are trapped in regions of negative ζ_g, where they rapidly propagate into the thermocline. These anticyclonic-rotating regimes coincided with distribution of reduced OML cooling, as rapid downward dispersion of near-inertial energy reduced the amount of kinetic energy available to increase vertical shears at the OML base. By contrast, forced OML near-inertial waves were stalled in upper layers of cyclonic circulations, which strengthened vertical shears and entrainment cooling. Upgoing near-inertial energy propagation dominated inside a geostrophic cyclone that interacted with Katrina; the salient characteristics of these upward propagating waves were: (i) radiated from the ocean interior due to geostrophic adjustment following the upwelling and downwelling processes; (ii) rather than with the buoyancy frequency, they amplified horizontally as they encountered increasing values of during upward propagation; (iii) produced episodic vertical mixing through shear-instability at a critical layer underneath the OML. To improve the prediction of TC-induced OML cooling, models must capture geostrophic features; and turbulence closures must represent near-inertial wave processes such dispersion and breaking between the OML base and the thermocline. Oceanic response models must capture this variability to get the correct entrainment in cold and warm oceanic features. For the first time, these effects of the near-inertial wave wake in the presence of a background eddy field are now being explored in this study using these measurements and results from analytical theory.

To examine the observed levels of cooling in the WCE (~0.5 to 1°C) and CCE (~4°C), we used the predecessor of the HYCOM model (e.g, Miami Isopycnic Coordinate Ocean Model, or MICOM) to reduce spurious vertical mixing in a highly idealized configuration. Isopycnic coordinate models suppress the spurious numerical dispersion of material and thermodynamic properties. MICOM consists of four prognostic equations for the horizontal velocity vector, mass continuity or layer thickness tendency, and two conservative equations for salt and heat (Bleck and Chassignet, 1994). A modified version of MICOM (Chérubin *et al.*, 2006) is used to include a fourth-order scheme for the non-linear advective terms in the momentum equations and biharmonic horizontal diffusion. This modified version reduces numerical noise associated with dispersive effects and the development of shocks in frontal regimes. The model approach used in Jaimes *et al.* (2011) is:

1) Buoyancy fluxes are ignored both in the density equation and in the turbulent kinetic energy (TKE) equation (for consistency) because the interest is to isolate the OML response due to internal oceanic processes, which have been proven to drive most of the

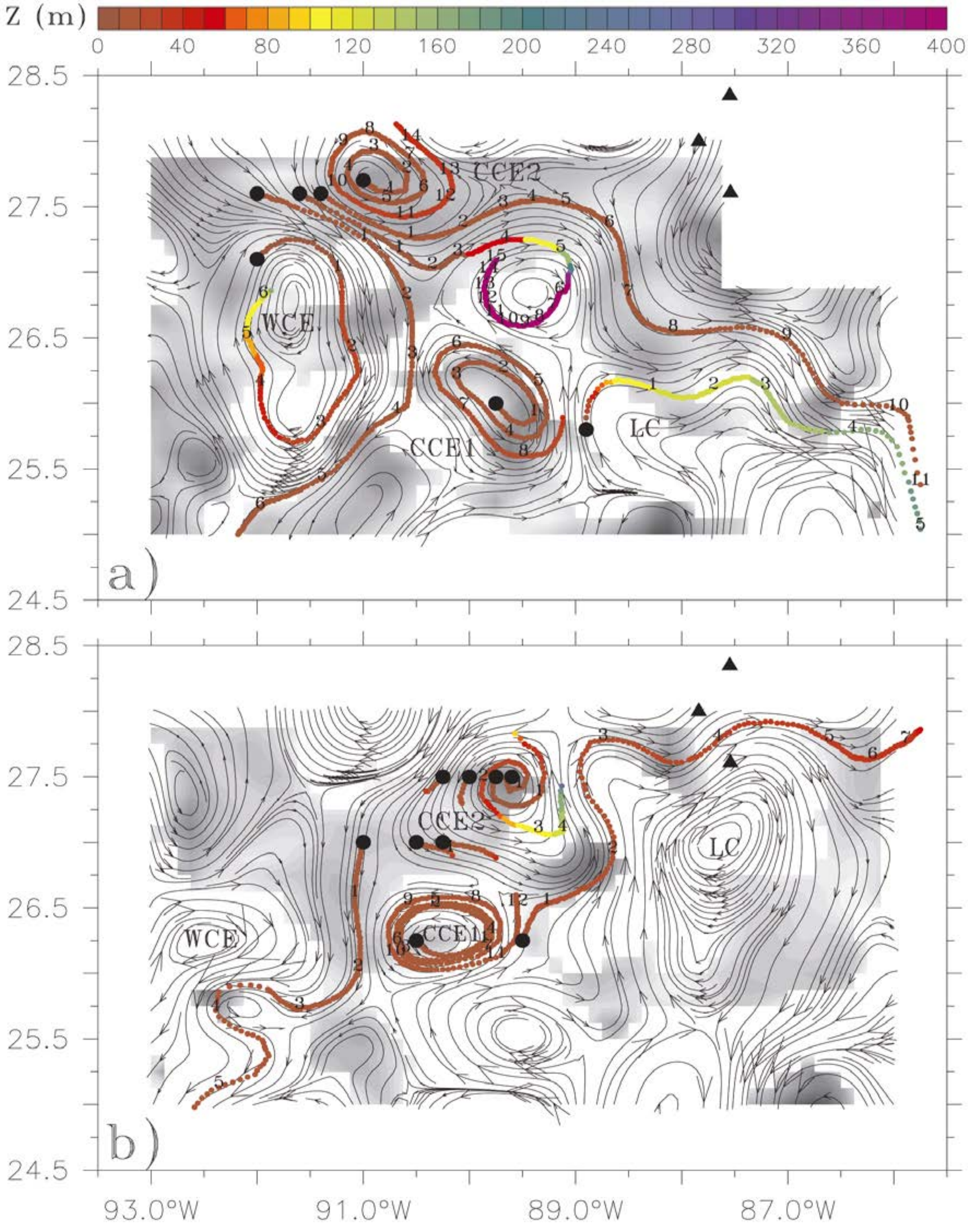

Figure. 13: *Near-inertial wave ray-tracing based on Kunze's (1985) model, for (a) Katrina and (b) Rita. The numbers along the wave rays indicate inertial periods (one inertial period is ~25.5 hr), dots are hourly positions, color is the ray's depth level, and the flow lines are from geostrophic flow fields derived from (a) post Katrina (15 Sept.) and (b) post Rita (26 Sept.) airborne-based data. The gray shades represent regions where the effective Coriolis parameter exceeds > 0.2. This ratio and the flow lines were calculated from depth-averaged velocity fields.*

TC-induced OML cooling (Price, 1981; Greatbatch, 1984; Shay *et al.*, 1992; Jacob *et al.*, 2000; Hong *et al.*, 2000; Shay and Brewster ,2010).

2) The turbulence closure for the OML only considers: (i) instantaneous wind erosion by the wind-driven frictional velocity (Kraus and Turner, 1967 :KT); and, (ii) vertical shear-driven entrainment at the OML base and over the stratified ocean below (Price *et al.*, 1986: PWP). These turbulence closures were chosen by reason of their mathematical simplicity, and because they provide direct physical insight on important mixing process observed over the thermocline inside a CCEs impacted by Katrina (JS09; JS10).
3) Idealized vortices (WCEs and CCEs) are initialized with an analytical model and density structures from direct measurements obtained during Katrina and Rita; these vortices satisfy the QG approximation.
4) An *f*-plane is used to prevent self-propagation of the QG vortices, which facilitates analyzing the near-inertial response at fixed points inside the stationary vortex. This approach cancels horizontal dispersion of near-inertial oscillations (NIOs) by meridional gradients in planetary vorticity (Gill, 1984). Any resulting horizontal wave dispersion is purely driven by ζ_g.

The computational domain is a 2000×2000 km square ocean with an initially circular QG vortex (WCE or CCE) of ~150 to 300 km in diameter located at the center. The vertical extension of the vortex is 950 m, representative of Gulf of Mexico's WCEs and CCEs The vortex is located on top of an initially quiescent layer of 4000 m in thickness. The bottom is flat, and lateral boundary conditions are closed. The central latitude of the domain is 26.9^{o}N, which allows reproducing near-inertial responses at the latitude of moorings used in JS09 and JS10. The horizontal grid resolution is 10 km that allows the resolution of horizontal wavelengths larger than 20 km. Horizontal resolutions of ~10 km are adequate for these investigations (Halliwell *et al*., 2011).

Three vertical resolutions were used: 12, 23, and 47 isopycnic layers (Figure 14). In every case, the model's top layer represents the OML. The initial OML thickness is the same for every vertical resolution, and it is determined by the analytical model as a function of the radius of the vortex, the target maximum azimuthal velocity, and density profiles from observational data. Given that experiments with higher vertical resolution improve the representation of the stratified ocean below the OML, OML cooling, and vertical dispersion of near-inertial energy, the discussion focus on the 47-layer numerical experiments that have vertical resolution of 10 m between the OML and the thermocline, allowing the model to resolve vertical wavelengths larger than 20 m. (The vertical sampling grid in the moorings used in Jaimes and Shay (2009, 2010) is ~8 m.)

Table 3: *Characteristics of geostrophic features in the Gulf of Mexico where LC represents a clockwise-rotating ocean feature where U, L, OML and Ro represent current, diameter, ocean mixed layer depth, and Rossby number of the warm and cold eddies, respectively.*

	Observed		Modeled			
Parameter	LC/WCE	CCE	WCE1	WCE2	CCE1	CCE2
U [m s^{-1}]	1–2	0.5–0.8	0.95	1.5	0.6	0.8
L [km]	200–400	100–150	250	300	150	150
OML [m]	~80	~30	~65	~80	~30	~25
Ro (U/*f* L)	0.05–0.1	0.05–0.08	0.06	0.08	0.06	0.08

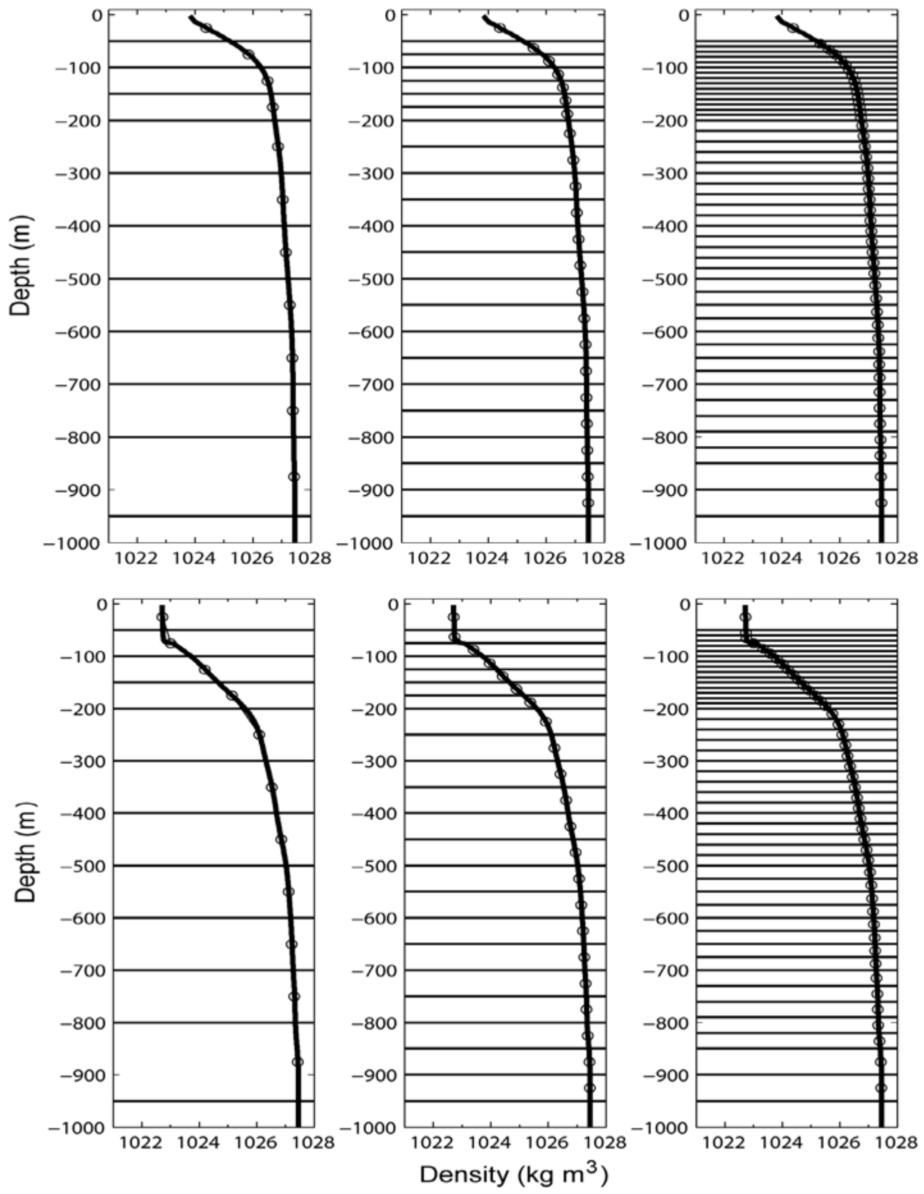

Figure 14: *Model isopycnic layers: 12, 23, and 47, from left to right panels. Upper (lower) panels are for CCEs (WCEs). The circles represent the model density, and the bold line is the observed density profile (smoothed via polynomial fit). The horizontal lines represent the initial layer thickness outside the QG vortex. The top layer is the OML, and the bottom layer is not shown.*

Based on observed characteristics of Gulf of Mexico's WCEs and CCEs, four eddies are reproduced (Table 3): WCE1 (Ro=0.06), WCE2 (Ro=0.08), CCE1 (Ro=0.06), and CCE2 (Ro=0.08). These vortices are initialized in model runs with parameters summarized in Table 3. The main focus is on CCE2 and WCE1, because these model vortices are similar to eddy features that interacted with Katrina (CCE) and Rita (LC bulge). For these cases, the incorporation of vertical shear-driven mixing parameterization (R_b=1 in PWP), reproduced additional average OML cooling of about 0.1^{o}C on the right side of the storm track inside WCE1 (Fig. 15a, c). Maximum cooling of about 0.7^{o}C was reproduced by KT+PWP in the vicinity of the moorings, compared with maximum cooling of ~0.5^{o}C by KT. The small difference between KT and KT+PWP indicates that in this warm anticyclone most of the cooling was driven by instantaneous wind erosion, and near-inertial vertical shear was not an important cooling mechanism, in accord with observational evidence presented elsewhere (Shay and Uhlhorn, 2008; JS09; JS10). In the case of CCE2, PWP caused additional cooling of more than 1.2^{o}C that confirms the importance of near-inertial vertical shears for OML cooling in this oceanic cyclone (Fig. 15b, d). Inside CCE2, near-inertial vertical shear instability impacted both the magnitude of the cooling, and the horizontal extension of the region of cooling. These results are consistent with the observed cooling during Katrina and Rita in the LC and WCE (Jaimes and Shay 2009, 2010).

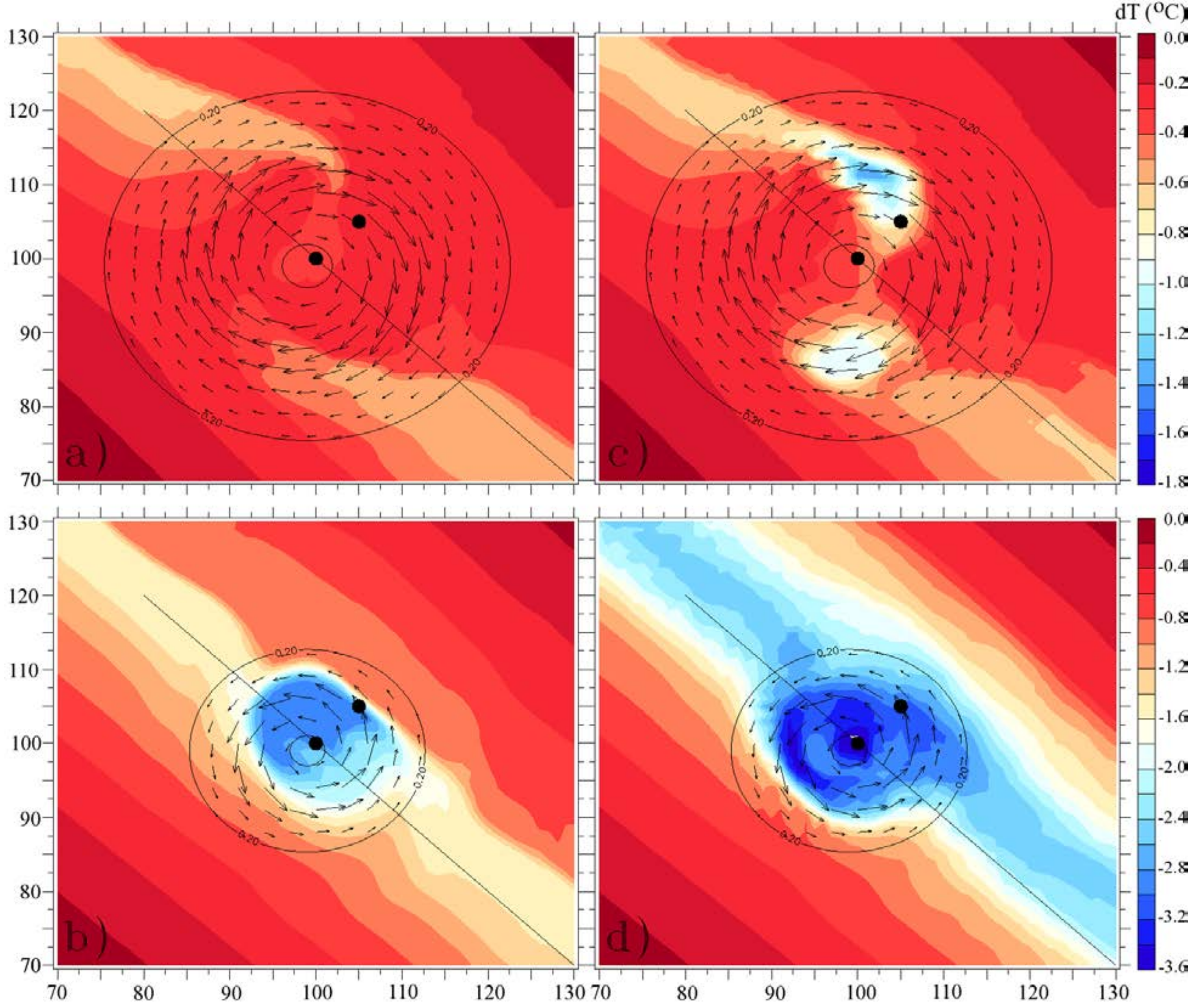

Figure 15. *OML cooling dT (^{o}C) in WCE1 (upper panels) and CCE2 (lower panels), in terms of the KT turbulence closure (a and b), and KT+PWP (c and d), where* $dT = T(\mathrm{IP} = 3) - T(\mathrm{IP} = -1.5)$. *Notice the difference in temperature scale between upper and lower panels. Vectors represent pre-storm currents in the OML and black line is trajectory of an idealized storm moving at 6 m s^{-1} (from Jaimes et al., 2011).*

Gustav and Ike: Hurricanes Gustav and Ike moved over the Gulf of Mexico and interacted with the LC and the eddy field in August and September 2008 (Meyers, 2011). As part of the NCEP tail Doppler Radar Missions, oceanic and atmospheric measurements were acquired on sixteen NOAA WP-3D research flights for pre, during and post-storm flights. In total, over 400 AXBTs and 200 GPS sondes were deployed to document the evolving atmospheric and oceanic structure over warm and cooler ocean features in these two hurricanes (Table 4). In addition, forty-five

GPS sondes were deployed on 1 Sept over the float and drifter array deployed by the United States Air Force WC-130J north and west of the Loop Current. Similar to CBLAST observations, the float array also included the EM/APEX floats that measure the horizontal velocities as well as temperature and salinity structure (Sanford *et al*., 2007). However, this effort significantly improved upon the CBLAST effort in that the forcing is better documented with the combination of GPS sondes and the Stepped Frequency Microwave Radiometer (Uhlhorn *et al.,* 2007) directly over the float and drifter array. In addition, each research flight carried AXBTs to document the evolving upper ocean thermal structure across the entire Gulf of Mexico for the first time. Note that the AXBTs were deployed to document pre- and post-storm oceanic variability in the Loop Current and its periphery where float and drifter measurements would be advected away from the storm track by the energetic ocean current. <u>This is precisely why we need current profilers to deploy from the research aircraft on a routine basis. As stated above, for Katrina and Rita, modeling studies of Gustav and Ike were also delayed until the new Navy ocean analysis product becomes available for initialization.</u>

Summary: While the grant began in 2007 and essentially ends with this final report, this study has been productive in combining both basic and applied research aimed at operational forecast models. A criticism of our work (more basic/applied research than operational implementation) has some validity as reflected in the comments on our recent proposal, however, oceanic and coupled model efforts have been ongoing for at least a decade at NCEP. Notwithstanding, we would argue that these "coupled" efforts have not systematically (and carefully) addressed key science issues related to the ocean models used to eventually couple to HWRF. Fundamentally, there has not been appropriate development of metrics to assess oceanic model performance within a consistent fluid dynamical framework such as Taylor (2001) diagrams discussed herein. Using data as our guide to modeling, we have emphasized the need for high quality ocean data needed for these evaluations. For example, we made significant progress on this grant from numerical simulations with complex oceanic conditions observed during hurricane Ivan's passage (Halliwell *et al.*, 2011), hurricane's Katrina and Rita (Jaimes *et al.,* 2011), and DWH Oil Spill disaster (Shay *et al.*, 2011).

With respect to oceanic impacts, intensity changes over warm and cold eddies represent regimes of less and more negative feedback to the atmosphere. Thus, the ocean is important in the coupled forecast problem. Accordingly, we have completed the analysis of Ivan within the context of mixing and upwelling and downwelling processes by comparing simulations of the currents and shears to *in situ* measurements from the SEED moorings (Teague *et al*., 2007). In addition, we have analyzed pre- Katrina and Rita observations including detailed ray-tracing techniques (Kunze, 1985) to demonstrate the markedly different character of the forced near-inertial motions (Jaimes and Shay, 2010). As well as mixing processes from idealized MICOM simulations (Jaimes *et al.,* 2011). We will conduct a similar analysis on the HYCOM simulations when realistic ocean conditions are available from the Navy reanalysis to assess the impact on the mixing schemes via shear-instability. Over the past four years, these combined numerical and observational efforts here have benefitted from students (E. Uhlhorn, B. Jaimes, P. Meyers) to examine model sensitivities and comparing these simulations to the various data sets.

During the summer of 2010, several near weekly flights in support of Deep Water Horizon Oil Spill certainly improved ocean model initialization through advanced data assimilation methods that must be transitioned to EMC as a warm eddy was shed from the LC over that three month period (Shay *et al.,* 2011). This is a regime where hurricanes can rapidly weaken or deepen as they interact with both warm and cold ocean features. Even under quiescent conditions, these data sets represent a challenge to the model to get the 3-D temperature, salinity and current structure accurately through vertical projection of the altimetry data. Processed profiler data from Gustav and Ike flights are being synthesized with drifter and float data to provide a clearer description of the cold wake northeast of the Loop Current where cooling exceeded 3^{o}C compared to the Loop Current of about 1^{o}C. Finally, we note that the Navy is now in the process of running a HYCOM global ocean reanalysis from 1993 to the present using the new vertical projection method. The reduced errors and biases expected with this reanalysis (see Figure 8) will enable us to evaluate model performance for earlier storms (time permitting) without the large negative impact of the cold bias that previously limited our ability to evaluate and improve ocean model parameterizations. The analysis will also benefit from the 5-year BOEMRE Loop Current Dynamics Study that includes extensive in situ measurements.

Table 4: *Summary of atmospheric (GPS) and oceanic (AXBT) profiler measurements from sixteen flights acquired in hurricanes Gustav and Ike in 2008. Numbers in parentheses represent profiler failures.*

Hurricane Gustav				Hurricane Ike			
Date	Flight	GPS	AXBT	Date	Flight	GPS	AXBT
(2008)				(2008)			
28 Aug	RF43	0	49(2)	08 Sep	RF43	0	47(2)
29 Aug	RF42	12(4)	16(0)	09 Sep	RF42	19	6(0)
30 Aug	RF43	9	19(2)	10 Sep	RF42	17(1)	10(2)
31 Aug	RF42	24	16(1)	10 Sep	RF43	11	20(7)
31 Aug	RF43	17(2)	19(1)	11 Sep	RF42	16	10(1)
01 Sep	RF43	44	19	11 Sep	RF43	10	22(3)
03 Sep	RF43	4	54(4)	12 Sep	RF42	21(2)	10(4)
				12 Sep	RF43	8	20(4)
				15 Sep	RF43	0	61(5)
Total	7	111(6)	191(10)		9	111(3)	216(28)

Acknowledgments: This study has benefited from the interactions with Mr. William Teague in the Oceanography Department at the US Naval Research Laboratory at Stennis Space Center, Dr. Alexis Lugo-Fernandez at BOEMRE who provided ADCP moorings. This project has also benefited from support from the NSF, NASA, BOEMRE and NOAA (OR&R and OAR) in the acquisition and analysis of in situ and satellite measurements acquired during hurricanes and Deep Water Horizon oil spill in collaboration with NOAA's Hurricane Research Division (Drs. Frank Marks, Rob Rogers, Eric Uhlhorn) and Aircraft Operations Center (Dr. James McFadden, Capt. Brad Kearse). Dr. Benjamin Jaimes has also contributed to this effort.

References (* Represents Publications from Grant Support 2007-2011)

Bleck, R., and E. P. Chassignet, 1994: Simulating the oceanic circulation with isopycnic-coordinate models. *The Oceans: Physical-Chemical Dynamics and Human Impact*, S. K. Majumdar et al., Eds., The Pennsylvania Academy of Science, 17-39.

Chérubin, L. M., Y. Morel, and E. P. Chassignet, 2006: Loop Current ring shedding: The formation of cyclones and the effect of topography. *J. Phys. Oceanogr.*, **36**, 569–591.

Donelan, M. A., B. K. Haus, N. Reul, W. J. Plant, M. Stiassine, H. Graber, O. Brown, and E. Saltzman, 2004: On the limiting aerodynamic roughness of the ocean in very strong winds. *Geophys. Res. Letters*., **31L18306**,doi:1029/2004GRL019460.

Falkovich, A., I. Ginis, and S. Lord, 2005: Implementation of data assimilation and ocean initialization for the coupled GFDL/URI hurricane prediction system. *J. Atmos. and Ocean. Tech*., **22**, 1918–1932.

*Halliwell, G., L. K. Shay, S. D. Jacob, O. Smedstad, and E. Uhlhorn, 2008: Improving ocean model initialization for coupled tropical cyclone forecast models using GODAE nowcasts. *Mon. Wea Rev*., **136 (7),** 2576–2591.

*Halliwell, G. R., L. K. Shay, J. Brewster, and W. J. Teague, 2011: Evaluation and sensitivity analysis to an ocean model response to hurricane Ivan. *Mon. Wea. Rev*., **139**, 921-945.

Hong, X., S. W. Chang, S. Raman, L. K. Shay, and R. Hodur, 2000: The interaction between Hurricane Opal (1995) and a warm core ring in the Gulf of Mexico. *Mon. Wea. Rev.*, **128**, 1347–1365.

Jacob, S. D., L. K. Shay, A. J. Mariano, and P. G. Black, 2000: The 3D mixed layer response to Hurricane Gilbert. *J. Phys. Oceanogr*., **30**, 1407–1429.

*Jaimes, B., 2009: On the oceanic response to tropical cyclones in mesoscale ocean eddies. PhD Dissertation. Division of Meteorology and Physical Oceanography, Rosenstiel School of Marine and Atmospheric Science, University of Miami, Coral Gables, FL 33134, 143 pp.

*Jaimes, B. and L. K. Shay, 2009: Mixed layer cooling in mesoscale eddies during Katrina and Rita. *Mon. Wea. Rev*., **137**, 4188–4207.

*Jaimes, B. and L. K. Shay, 2010: Near-inertial wave wake of hurricanes Katrina and Rita in mesoscale eddies. *J. Phys. Oceanogr*.. .**40,** 1320-1337.

*Jaimes, B., L. K. Shay, and G. R. Halliwell, 2011: The response of quasi-geostrophic oceanic vortices to tropical cyclone forcing. *J. Phys. Oceanogr*., **41**, doi:10.1175/JPO-D-11-06.1, (*In Press*).

Jarosz, E., D. A. Mitchell, D. W. Wang, and W. J. Teague, 2007: Bottom-up determination of air-sea momentum exchange under a major tropical cyclone. *Science*, **315**, 1707-1709.

Kraus, E. B., and J. S. Turner, 1967: A one-dimensional model of the seasonal thermocline. II: The general theory and its consequences, *Tellus*, **19**, 98-105.

*Mainelli, M., M. DeMaria, L. K. Shay and G. Goni, 2008: Application of oceanic heat content estimation to operational forecasting of recent category 5 hurricanes, *Wea and Forecast*., **23(1),** 3-16.

*Meyers, P. C., 2011: Development and analysis of the Systematically Merged Atlantic Regional Temperature and Salinity (SMARTS) climatology for satellite-derived ocean thermal structure. M. S. Thesis, University of Miami, Coral Gables, FL, 33134, 99 pp.

Murphy, A. H., 1988. Skill scores based on the mean square error and their relationships to the correlation coefficient. *Mon. Wea. Rev.*, **116**, 2417-2424.

Nowlin, W. D. Jr., and J. M. Hubertz, 1972: Contrasting summer circulation patterns for the eastern Gulf. In: Contributions on the Physical Oceanography of the Gulf of Mexico, *Texas A&M Oceanogr. Stud.*, **vol. 2**, edited by L. R. A. Capurro and J. L. Reid, pp. 119-138, Gulf Pub. Co.

Price, J. F., R. A. Weller, and R. Pinkel, 1986: Diurnal cycling: Observations and models of the upper ocean response to diurnal heating, cooling, and wind mixing. *J. Geophys. Res.*, **91(C7),** 8411-8427.

Powell, M. D., P. J. Vickery, and T. A. Reinhold, 2003: Reduced drag coefficient for high wind speeds in tropical cyclones. *Nature*, **422**, 279-283.

Reynolds, R. W., T. M. Smith, C. Liu, D. B. Chelton, K. S. Casey, and M. G. Schlax, 2007: Daily high-resolution blended analyses for sea surface temperature. *J. Climate*, **20**, 5473-5496.

Rogers, R., S. Aberson, M. Black, P. Black, J. Cione, P. Dodge, J. Dunion, J. Gamache, J. Kaplan, M. Powell, L. K.Shay, N. Surgi, E. Uhlhorn, 2006: The intensity forecasting experiment (IFEX), a NOAA multiple year field program for improving intensity forecasts. *BAMS*, **87(11),** 1523-1537.

*Rappaport, E. N., J. L. Franklin, M. DeMaria, A. B. Shumacher, L. K. Shay and E. J. Gibney, 2010: Tropical cyclone intensity change before U. S. Gulf coast landfall. *Wea. and Forecast*., **25,** 1380-1396.

Sanford, T B., J. F. Price, J. Girton, and D. C. Webb, 2007: Highly resolved observations and simulations of the oceanic response to a hurricane. *Geophys. Res. Lett*., **34**, L13604, 5 pp.

*Shay, L.K., 2009: Upper Ocean Structure: a Revisit of the Response to Strong Forcing Events. *In: Encyclopedia of Ocean Sciences*, ed. John Steele, S.A. Thorpe, Karl Turekian and R. A. Weller, Elsevier Press International, Oxford, UK, 4619-4637, doi: 10.1016/B978-012374473-9.00628-7.

*Shay, L. K., 2010: Air-Sea Interactions in Tropical Cyclones (Chapter 3). In Global Perspectives of Tropical Cyclones, 2nd Edition, Eds. Johnny C. L. Chan and J. D. Kepert, *World Scientific Publishing Company*: Earth System Science Publication Series, London, UK, 93-131.

*Shay, L. K., 2010: Air-sea interface and oceanic influences (Chapter 1.3). *Topic Chairman and Rapporteurs Report for Tropical Cyclone Structure and Structure Change of the 7th WMO International Workshop on Tropical Cyclones (IWTC-7) 15-21 Nov 2010 in St. Denis, La ReUnion,* France, World Meteorological Organization Tropical Meteorology Research Series, ***WMO TD-1561***, Eds.C. Velden, and J. Kepert, Geneva, Switzerland, 48pp.

*Shay, L. K., B. Jaimes, J. K. Brewster, P. Meyers, C. McCaskill, E. W. Uhlhorn, F. D. Marks, G. R. Halliwell, O. M. Smedsted and P. Hogan, 2011: Airborne surveys of the Loop Current complex from NOAA WP-3D during the Deep Water Horizon oil spill. Eds, Y. Liu and D. Streets, AGU Monograph Special Issue, Monitoring and Modeling Deep Water Horizon Oil Spill, (*In Press)*

Shay, L. K., A. J. Mariano, S. D. Jacob, and E. H. Ryan, 1998: Mean and near-inertial response to hurricane Gilbert. *J. Phys. Oceanogr.*, **28**, 858–889.

*Shay, L. K. and E. Uhlhorn, 2008: Loop Current Response to hurricanes Isidore and Lili, *Mon. Wea. Rev.*, **137,** 3248-3274.

*Shay, L. K., and J. Brewster, 2010: Oceanic heat content variability in the eastern Pacific Ocean for hurricane intensity forecasting. *Mon. Wea. Rev*., **138(6),** 2110-2131..

Taylor, K. E., 2001: Summarizing multiple aspects of model performance in a single diagram. *J. Geophys. Res*., **106**, 7183-7192.

Teague, W. J., E. Jarosz, D. W. Wang, and D. A. Mitchell, 2007: Observed oceanic response over the upper continental slope and outer shelf during Hurricane Ivan, *J. Phys. Oceanogr.* **37**, 2181-2206.

Uhlhorn, E. W., P. G. Black, J. L. Franklin, M. Goodberlet, J. Carswell and A. S. Goldstein, 2007:Hurricane surface wind measurements from an operational stepped frequency microwave radiometer. *Mon. Wea. Rev*., **135**, 3070-3085.

*Uhlhorn, E. W., 2008: Gulf of Mexico Loop Current mechanical energy and vorticity response to a tropical cyclone. PhD Dissertation. RSMAS, University of Miami, Coral Gables, FL 33143, 148 pp.

*Uhlhorn, E., and L. K. Shay, 2011: Loop Current mixed layer response to hurricane Lili (2002) Part I: Observations. *J. Phys. Oceanogr.* (*Accepted subject to minor revision*)

*Uhlhorn, E., and L. K. Shay, 2011: Loop Current mixed layer response to hurricane Lili (2002) Part II: Modeling results. *J. Phys. Oceanogr.* (*Submitted*)

Walker, N., R. R. Leben, and S. Balasubramanian, 2005: Hurricane forced upwelling and chlorophyll a enhancement within cold core cyclones in the Gulf of Mexico. Geophys. *Res. Letter*, **32**, L18610, doi: 10.1029/2005GL023716, 1-5.